Single-color centers implanted in diamond nanostructures

2011 New J. Phys. 13 045004

(http://iopscience.iop.org/1367-2630/13/4/045004)

New Journal of Physics
The open-access journal for physics

Single-color centers implanted in diamond nanostructures

Birgit J M Hausmann[1,5], Thomas M Babinec[1,5], Jennifer T Choy[1,5], Jonathan S Hodges[2,3,4], Sungkun Hong[2], Irfan Bulu[1], Amir Yacoby[2], Mikhail D Lukin[2] and Marko Lončar[1,6]

[1] School of Engineering and Applied Sciences, Harvard University, Cambridge, MA 02138, USA
[2] Department of Physics, Harvard University, Cambridge, MA 02138, USA
[3] Department of Nuclear Science and Engineering, Massachusetts Institute of Technology, Cambridge, MA 02139, USA
[4] Department of Electrical Engineering, Columbia University, New York, NY 10027, USA
E-mail: loncar@seas.harvard.edu

New Journal of Physics **13** (2011) 045004 (11pp)
Received 21 September 2010
Published 5 April 2011
Online at http://www.njp.org/
doi:10.1088/1367-2630/13/4/045004

Abstract. The development of material-processing techniques that can be used to generate optical diamond nanostructures containing a single-color center is an important problem in quantum science and technology. In this work, we present the combination of ion implantation and top-down diamond nanofabrication in two scenarios: diamond nanopillars and diamond nanowires. The first device consists of a 'shallow' implant (∼20 nm) to generate nitrogen-vacancy (NV) color centers near the top surface of the diamond crystal prior to device fabrication. Individual NV centers are then mechanically isolated by etching a regular array of nanopillars in the diamond surface. Photon anti-bunching measurements indicate that a high yield (>10%) of the devices contain a single NV center. The second device demonstrates 'deep' (∼1 μm) implantation of individual NV centers into diamond nanowires as a post-processing step. The high single-photon flux of the nanowire geometry, combined with the low background fluorescence of the ultrapure diamond, allowed us to observe sustained photon anti-bunching even at high pump powers.

[5] These authors contributed equally to this work.
[6] Author to whom any correspondence should be addressed.

Contents

1. Introduction

The development of robust and practical quantum information processing systems is an important problem at the interface between materials science, photonics and atomic physics. Light-emitting defects (color centers) in diamond are increasingly attractive for their implementation in a solid-state platform. For example, color centers based on nitrogen [1]–[3], silicon [4], carbon [5], nickel [6] and chromium [7] impurities have been shown to generate non-classical states of light and emit single photons at room temperature, which is a critical resource for quantum optical communication systems. Of these defects, the nitrogen-vacancy (NV) center is very attractive since it can possess additional electron and nuclear spin degrees of freedom with long coherence times that act as a quantum memory for long-distance quantum communications [8, 9], quantum computing [10]–[14] and nanoscale magnetometry [15]–[17]. Efforts to identify other outstanding color centers in diamond are ongoing [18].

Practical implementations of these technologies require the integration of single-color centers into diamond photonic systems whose optical performance exceeds that offered by a homogeneous bulk diamond crystal. Towards this end, a variety of photonic devices are under development that: (i) enable efficient single-photon collection and overcome total internal reflection at the diamond–air interface and (ii) engineer optical properties such as fluorescence spectrum and lifetime of an individual NV center. Some of these devices are based on broad-band antenna [3, 19] or solid immersion lens [20] effects, while others are based on narrow-band cavity resonance enhancements [21]–[26]. Concurrently, there has been interest in engineering the spatial distribution of single-color centers in diamond via ion implantation on a large scale. Techniques based on blanket implantation at different dosages [27, 28], focused ion implantation [29] and implantation through nanoscale apertures [30, 31] have all been demonstrated to generate single-color centers in a bulk crystal. Future scalable quantum technologies will benefit from complete fabrication routines that combine diamond photonic device engineering with ion implantation of color centers at the single defect level.

In this paper, we demonstrate two complementary procedures that are widely applicable to quantum photonic devices based on diamond: implantation of single-color centers before and after top-down diamond nanofabrication. In section 2, we demonstrate the ability to generate large arrays of diamond nanopillars near the top surface of the diamond crystal via a low-energy, ‘shallow’ implantation of nitrogen followed by dry etching. This scalable fabrication technique could be used to facilitate the coupling of single NV centers to proximal nanophotonic devices in the future. In section 3, we demonstrate the ability to perform a high-energy, ‘deep’ implantation of nitrogen at a low density into large arrays of diamond nanowires that have been fabricated from a bulk crystal. An NV center in the nanowire acts as a high-flux source

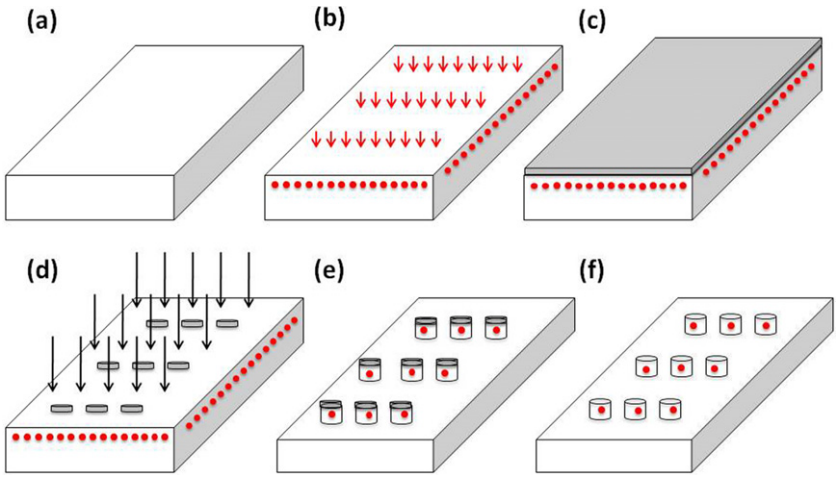

Figure 1. Approach to isolate-implanted NV centers in large arrays of diamond nanopillars fabricated in a high-purity single-crystal diamond substrate: (a) start with clean type-IIa diamond, (b) low-energy nitrogen ion implantation plus annealing activate a thin surface layer of NV centers, (c) deposit electron beam lithography resist on the diamond surface, (d) electron beam lithography defines an etch mask, (e) reactive ion etching mechanically isolates individual NV centers in the device and finally (f) HF wet etch of the diamond reveals the structures.

of single photons due to an antenna effect that modifies its radiation pattern [3, 32], and the pure diamond host generates a low level of background fluorescence compared to previously demonstrated nanowire devices in type-Ib material. These combined effects enable photon anti-bunching to be observed at high pump powers, where single-photon count rates are maximized. In section 4, we discuss some natural extensions of these fabrication routines to future quantum photonic systems.

2. Fabrication and characterization of diamond nanopillars

Figure 1 shows our approach to realize the diamond nanopillar arrays studied in this experiment. First, high-quality electronic grade type-IIa diamond (element 6) grown in a chemical vapor deposition (CVD) chamber with low (<5 ppb) background nitrogen content was implanted with ^{15}N ions at an energy of 14 keV and a dosage of 1.25×10^{12} cm^{-2}. Stopping range of ions in matter (SRIM) calculations [33] project a nitrogen layer $\sim$20 nm below the diamond surface. Next, the sample was annealed at 750 °C for 2 h in high vacuum ($<10^{-6}$ Torr) to mobilize vacancies and generate a shallow layer of NV centers. Arrays of circular shaped masks (XR electron beam resist, Dow Corning) with $\sim$65 nm radius were then defined on the top surface using an electron beam lithography tool (Elionix). An oxygen dry etch, whose conditions were similar to those described elsewhere [32], was applied for 1 min and generated $\sim$200 nm-tall pillars on the top of the diamond surface. Finally, the sample was placed in a hydrofluoric acid wet etch for approximately 20 s to remove the residual mask layer and then in a 1 : 1 : 1 mixture of sulfuric, nitric and perchloric acid at 400 °C for $\sim$30 min to clean the sample. A scanning electron micrograph (SEM) of a typical nanopillar array is presented in figure 2(a).

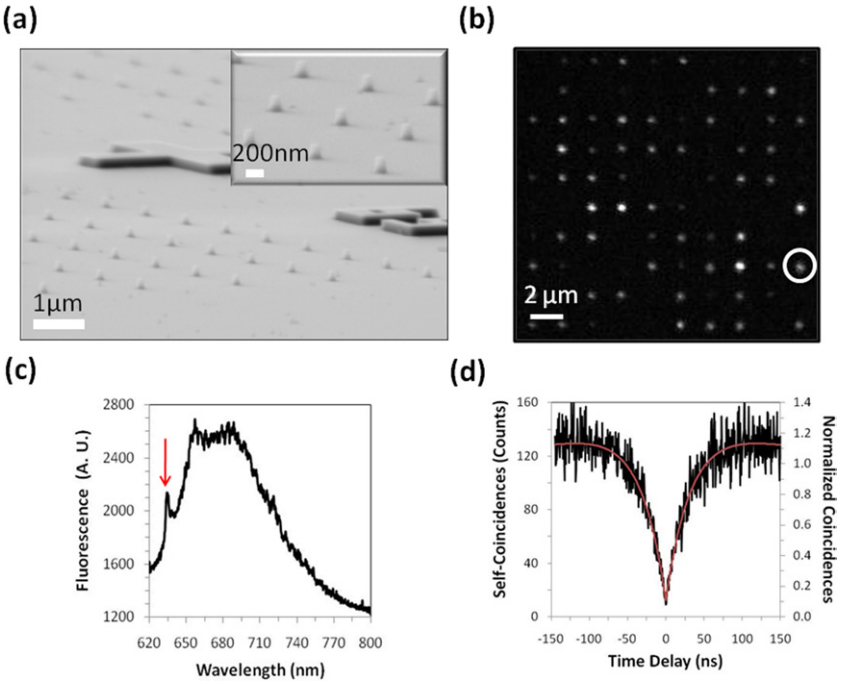

Figure 2. (a) SEM image of the array of nanopillars of height ∼200 nm and radius ∼65 nm. The inset shows a close-up of several pillars. (b) Confocal microscope image of a 10×10 array of diamond nanopillars, with center-to-center spacing of 2 μm (c) Photoluminescence spectrum of the nanopillar circled in (b). The ZPL of this device, indicated by an arrow, is at ∼634 nm. (d) Intensity autocorrelation function of the fluorescence emitted from the device circled in (b) shows photon anti-bunching with $g^{(2)}(0) \sim 0.08$, without any background subtraction, due to the presence of a single embedded NV center.

The sample was then characterized with a home-built confocal microscope system as described elsewhere [3]. An image of the fluorescence emitted under 532 nm continuous-wave (CW) excitation is presented in figure 2(b). It shows a 10×10 square array of bright spots that correspond to the nanopillar devices shown in figure 2(a), and the observed variation in the overall intensities results from the random embedding process that couples an NV center into each device. Measurements of their photoluminescence spectra show the characteristic zero-phonon line (ZPL) as well as broad phonon sideband of an embedded NV center (figure 2(c)). In most cases, however, significant deviation was observed in the position of the ZPL from its characteristic value of 637 nm in a bulk diamond sample. This appears to be consistent with reported ZPL shifts for diamond nanocrystals [34].

We then quantified the number of NV centers embedded inside individual nanopillar devices in this same array. In general, the number of quantum emitters may be obtained from measurements of the fluorescence intensity autocorrelation function $g^{(2)}(\tau) = \langle I(t)^* I(t+\tau)\rangle / \langle I(t)\rangle^2$ using a beam-splitter, two single-photon counting avalanche photodiodes (Perkin Elmer) and a time-to-amplitude converter (PicoHarp) in the Hanbury Brown and Twiss configuration [1]. This $g^{(2)}(\tau)$ function is obtained from the number of self-coincidences C.C.(τ) as a function of delay time τ according to $g^{(2)}(\tau) = \text{C.C.}(\tau)/(R_1 R_2 w T)$, where

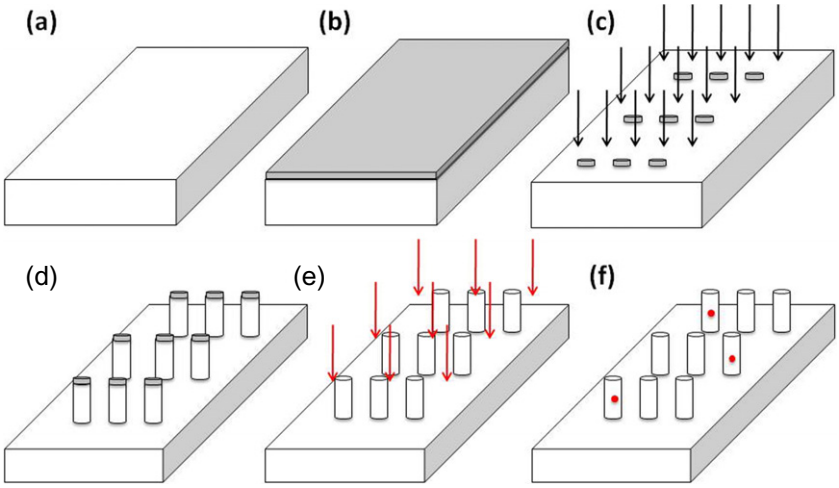

Figure 3. Approach to implant individual NV centers in large arrays of diamond nanowire antennas made from high-purity single-crystal diamond: (a) start with clean type-IIa diamond, (b) deposit electron beam lithography resist on the diamond surface, (c) electron beam lithography defines an etch mask, (d) HF wet etch of the diamond reveals the structures, (e) high-energy ion implantation of nitrogen and finally (f) annealing activates NV centers.

R_1 and R_2 are the photon count rates on channels 1 and 2, respectively, w is the bin width and T is the integration time. No background subtraction was performed. A single NV center cannot emit two photons at the same time, and the number of self-coincidence counts at zero delay, $g^{(2)}(0)$, is therefore expected to be zero in the absence of any sources of background fluorescence (e.g. surface contamination, impurities). The observed contrast decreases according to the formula $g^{(2)}(0) = 1–1/N$ for additional emitters N. Ten of the 17 devices that we tested showed strong photon anti-bunching $g^{(2)}(0) < 0.5$ (figure 2(d)), which indicates that the nanopillar contains a single NV center. The other seven devices were characterized by $0.5 < g^{(2)}(0) < 0.7$, which is consistent with the presence of two or three NV centers in the device.

There are several conclusions that we may draw from these results. Firstly, the anti-bunching data make it clear that background fluorescence generated by our processing technique is not prohibitively high for room-temperature studies of single-color centers. Secondly, since at least ten of the 100 total devices in this particular array contained a single NV center, this combined implantation and fabrication routine may be implemented with a high yield (>10%) operating in the single-photon regime. Finally, our high-throughput fabrication technique can generate many more devices than can be tested in serial with the standard confocal microscope system. This suggests the future need to develop automated characterization tools or wide-field microscope approaches that optically address many devices in parallel.

3. Fabrication and characterization of diamond nanowires

In this section, we modify the approach slightly and implant single NV centers in diamond nanowire antennas (figure 3). This geometry has recently been shown to offer significant enhancement in the excitation and extraction of single photons from an NV center compared

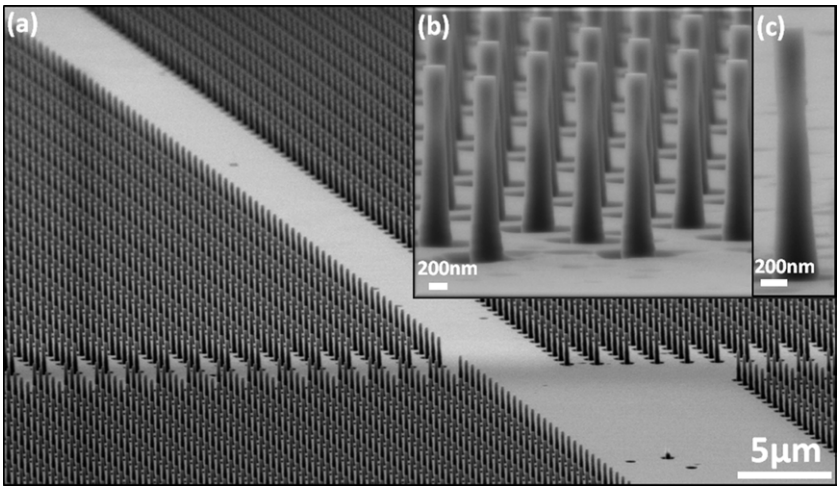

Figure 4. (a) SEM image of an array of nanowires of height $\sim 2\,\mu$m and diameter ~ 200 nm. Thousands of devices can be realized in parallel due to high-throughput nanofabrication techniques that were used. (b) and (c) Higher magnification images of nanowire arrays.

to bulk crystals due to the presence of an HE_{11} waveguide mode that efficiently collects input pump power and facilitates single-photon collection via vertical emission from the top facet [3, 32]. An SEM image of the sample shows large arrays with thousands of nanowire antennas of diameter ~ 200 nm and of height $\sim 2\,\mu$m fabricated in a single diamond chip (figure 4). The diamond nanowires were then implanted with ^{15}N at 1.7 MeV and 1×10^9 cm^{-2} dosage and annealed at 750 °C in high vacuum ($< 10^{-6}$ Torr) for 2 h. SRIM calculations indicate that this produces a layer of NV centers $\sim 1.0\,\mu$m below the diamond surface. The reduced dosage, used to potentially minimize implantation-related damage (important for future low-temperature studies), resulted in a relatively low yield of nanowires containing a single NV center.

In order to identify working devices, we scanned over large ($\sim 30 \times 30\,\mu$m) sections of the array at high powers (~ 3 mW) with a 532 nm CW laser. This allowed us to quickly bleach residual background fluorescence from the nanowire devices and observe sustained brightness in implanted devices due to the photostability of the NV center. Photoluminescence spectra did not exhibit the broad dispersion in the ZPL position that was observed in the nanopillar case, although some variation was observed from 637 to 639 nm. Figure 5 shows intensity auto-correlation measurements taken from one representative device at a series of increasing pump powers. Photon anti-bunching in the nanowire fluorescence $g^{(2)}(0) \sim 0.06$ was possible without background subtraction (figure 5(b)), which represents a fivefold reduction compared to nanowire devices demonstrated in type-Ib material [3]. In addition, photon anti-bunching $g^{(2)}(0) < 0.5$ is sustained at pump powers where the single-photon signal is saturated.

Contributions to the nanowire fluorescence come from single photons, S, that lead to non-classical correlations at zero time delay, as well as background fluorescence, B, emitted with Poisson statistics that reduces the observed contrast. For a given pump power, the relative contributions of S and B to the total fluorescence are encoded in the anti-bunching contrast according to [2] $g^{(2)}(0) = 1 - \rho^2$, where $\rho = S/(S + B)$. We therefore measured both the total number of photon counts per second from the nanowire as well as $g^{(2)}(0)$ for different pump

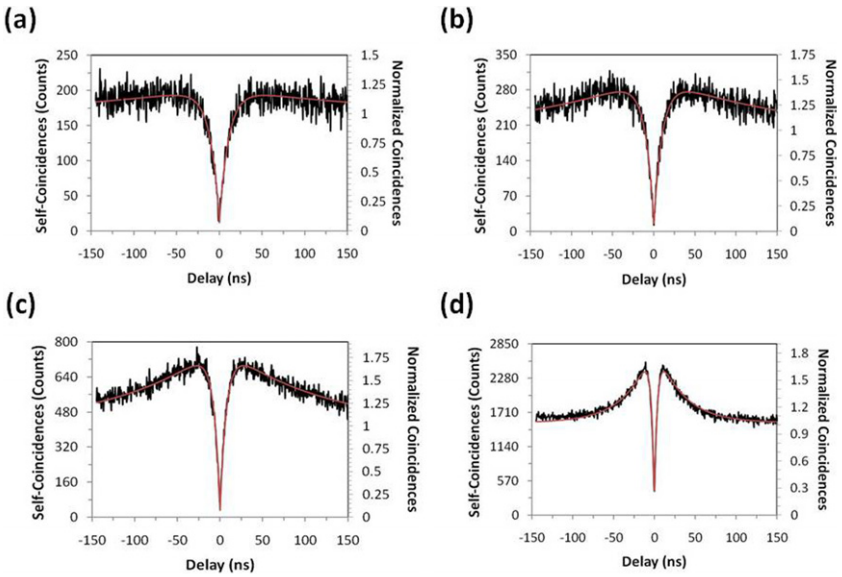

Figure 5. Intensity autocorrelation data for a single NV center implanted in a diamond nanowire shows sustained anti-bunching, without background subtraction, at increasing excitation powers due to high single-photon collection efficiency and low background. (a) 50 μW: $g^{(2)}(0) \sim 0.08$, (b) 100 μW: $g^{(2)}(0) \sim 0.06$, (c) 250 μW: $g^{(2)}(0) \sim 0.16$ and (d) 1000 μW: $g^{(2)}(0) \sim 0.27$. Pump power was measured before the microscope objective. Raw data (black) and theoretical fits (red) are shown.

powers P (figure 6(a)). The results are in good agreement with theoretical predictions (dashed line). The saturation curve for this device demonstrates that an implanted nanowire may act as a high-flux single-photon source (figure 6(b)). The number of single photons collected from the NV center in the nanowire was observed to turn on sharply at low pump powers and saturate at high powers according to the model [1] $S(P) = \frac{\mathrm{CPS_{Sat}}}{1+P_{\mathrm{Sat}}/P}$. The maximum possible number of photons collected per second was $\mathrm{CPS_{Sat}} = 304\,000$ and the NV center saturation power was $P_{\mathrm{Sat}} = 0.34$ mW. This is consistent with the efficient excitation and extraction of single photons from an NV center that was previously reported for type-Ib nanowire antennas in our confocal microscope system [3].

Additional information on the optical properties of an NV center in a diamond nanowire may be obtained by triggering the emission of single photons. We have constructed a versatile-pulsed excitation system for this task [35]. Ultrafast ($\sim$200 fs) pulses generated by a Ti : sapphire (Coherent Mira 800-F) laser were used to generate supercontinuum white light in a photonic crystal fiber (Newport, SCG-800). A pump wavelength of $\sim$800 nm maximized the overall spectral density at green wavelengths, which was then isolated using band-pass filters in the 510–540 nm wavelength range (Semrock), collected with an optical fiber and used as an excitation source for our confocal microscope. Since the radiative rate of an NV center in a diamond nanowire ($\sim$60–80 MHz) [3] is comparable to the fundamental repetition rate of the Ti : sapphire pulse train (76 MHz), an electro-optic modulator (ConOptics, Model 350) was used to reduce the repetition rate to $\sim$10.8 MHz prior to launching in the photonic crystal fiber.

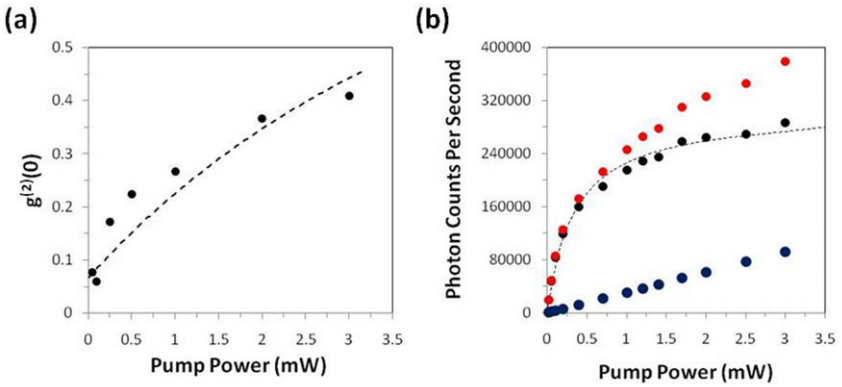

Figure 6. (a) $g^{(2)}(0)$ as a function of pump power. Data points correspond to the values of the normalized $g^{(2)}(0)$ data presented in figure 5. The dashed curve is the expected level of coincidence counts $1-\rho^2$ based on the measured saturation data presented in (b), where $\rho = S/(S+B)$, S is NV center single-photon count rate and B is background fluorescence count rate. (b) Total nanowire fluorescence from the same device is presented in red, the background fluorescence obtained from contrast in photon anti-bunching data in (a) is shown in blue and the remainder of the net single-photon counts from an embedded NV center is shown in black. A fit of the NV center fluorescence to the saturation model is given by the dashed black line. Pump power was measured before the microscope objective.

We used this excitation scheme to observe the full temporal dynamics of the diamond nanowire fluorescence. Pulsed intensity auto-correlation measurements show a series of spikes in coincidence counts at times separated by an integer number of laser repetition cycles (figure 7(a)). Strong suppression of the central peak $g^{(2)}(0) \sim 0.16$ is observed at 65 μW average pump power, which is consistent with the extent of the photon anti-bunching observed using CW excitation. Additionally, we were able to make a direct measurement of the exponential decay of the nanowire fluorescence after pulsed excitation (figure 7(b)). A fit was obtained from a bi-exponential function using a fast time constant $\tau_{bg} \sim 1.4 \pm 0.1$ ns, which corresponds to the decay of the background fluorescence, and a slow time constant $\tau_{nv} \sim 13.7 \pm 0.2$ ns, which corresponds to the fluorescence decay of the NV center in the nanowire. This value of τ_{nv} is consistent with previously reported values inferred from the width of the anti-bunching dip in CW studies of type-Ib nanowires [3].

4. Conclusions and future directions

We have demonstrated two novel techniques to implant color centers in diamond nanostructures, and both could be an important part of future solid-state quantum photonic systems. For example, embedding the nanopillar arrays presented in section 2 in a metal layer could allow for plasmon-enhanced single-photon emission [36]. These deterministically positioned nanopillars also offer convenient, evanescent coupling to other photonic crystal cavities in semiconductor material systems that have been proposed for cavity quantum electrodynamics studies [37]–[39]. In either case, the observed scalability provided by this system is an attractive resource for the development of more complex and integrated device architectures.

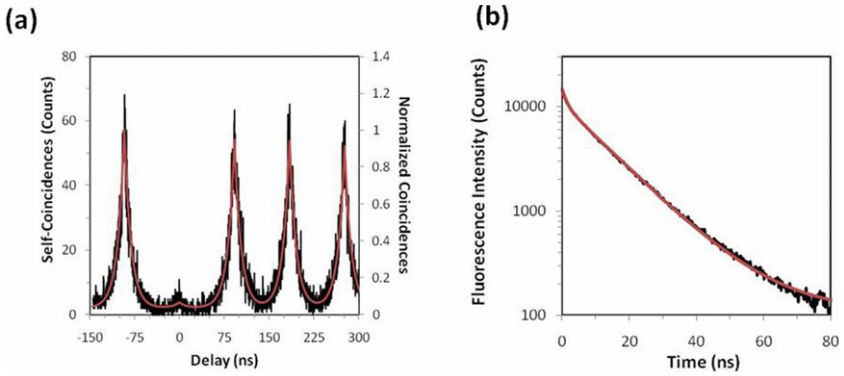

Figure 7. (a) Photon anti-bunching measurement of a diamond nanowire using pulsed excitation (65 μW average pump power). Strong suppression of the central peak at zero delay $g^{(2)}(0) \sim 0.16$ is observed without background subtraction. Raw data (black) and theoretical fit (red) are shown. (b) Measurement of the fluorescence lifetime via fluorescence decay is shown in black (14 μW average pump power). The red line corresponds to a bi-exponential fit to the fluorescence decay with time constants $\tau_{\mathrm{bg}} = 1.5$ ns for background fluorescence and $\tau_{\mathrm{nv}} = 13.7$ ns for the NV center fluorescence.

There are also several natural extensions of the deep implantation of NV centers into the nanowires shown in section 3. Ion implantation of other intrinsically brighter defects [7] into the nanowire devices is an exciting prospect. Moreover, the outstanding combination of high directionality of emission from the nanowire antenna combined with low background fluorescence in the pure diamond crystal has allowed us to observe anti-bunching $g^{(2)}(0) \sim 0.1$ in a confocal microscope system with reduced numerical aperture NA $\sim$0.6. We therefore anticipate that it will be possible to collect the NV center emission directly with a lensed optical fiber (NA $\sim$0.4) positioned above a nanowire. Finally, it is well known that at low temperatures the NV center ZPL can become transform limited in bulk type-IIa diamond samples [40], but that significant inhomogeneous broadening and spectral diffusion are typical in diamond nanocrystals [34]. Further low-temperature studies are therefore needed to investigate the impact of reactive-ion etching on the stability of NV centers (both natural and implanted ones) embedded within fabricated nanowires. Moreover, understanding the impact of ion implantation damage will also be an important issue in the future. Detailed studies on the optical transitions of implanted NV centers in diamond nanowire antennas will therefore be useful for understanding the broader role that diamond nanophotonics can play in quantum optics and information processing with NV centers.

Acknowledgments

We thank Patrick Maletinsky and Jero Maze for assistance with annealing the diamond used in this experiment, Fedor Jelezko and Helmut Fedder for helpful discussions about the implementation of the pulsed excitation system, and Daniel Twitchen from Element Six for helpful discussions and for diamond samples. TMB acknowledges support from the NDSEG and NSF fellowships, and JTC acknowledges support from the NSF graduate research

fellowship. ML acknowledges support from the Alfred P Sloan Foundation. Devices were fabricated in the Center for Nanoscale Systems (CNS) at Harvard. This work was supported in part by Harvard's Nanoscale Science and Engineering Center (NSEC), NSF NIRT grant (ECCS-0708905) and by the DARPA QuEST program.

References

[1] Kurtsiefer C, Mayer S, Zarda P and Weinfurter H 2000 Stable solid-state source of single photons *Phys. Rev. Lett.* **85** 290–3

[2] Beveratos A, Brouri R, Gacoin T, Poizat J-P and Grangier P 2001 Nonclassical radiation from diamond nanocrystals *Phys. Rev.* A **64** 061802(R)

[3] Babinec T M, Hausmann B J M, Khan M, Zhang Y, Maze J R, Hemmer P R and Loncar M 2010 A diamond nanowire single-photon source *Nat. Nano* **5** 195–9

[4] Wang C, Kurtsiefer C, Weinfurter H and Burchard B 2006 Single photon emission from SiV centres in diamond produced by ion implantation *J. Phys. B: At. Mol. Opt. Phys.* **39** 37–41

[5] Naydenov B, Kolesov R, Batalov A, Meijer J, Pezzagna S, Rogalla D, Jelezko F and Wrachtrup J 2009 Engineering single photon emitters by ion implantation in diamond *Appl. Phys. Lett.* **95** 181109

[6] Gaebel T, Popa I, Gruber A, Domhan M, Jelezko F and Wrachtrup J 2004 Stable single-photon source in the near infrared *New J. Phys.* **6** 98

[7] Aharonovich I, Castelletto S, Simpson D A, Stacey A, McCallum J, Greentree A D and Prawer S 2009 Two-level ultrabright single photon emission from diamond nanocrystals *Nano Lett.* **9** 3191–5

[8] Childress L, Taylor J M, Sorensen A S and Lukin M D 2006 Fault-tolerant quantum communication based on solid-state photon emitters *Phys. Rev. Lett.* **96** 070504

[9] Childress L, Taylor J M, Sorensen A S and Lukin M D 2005 Fault-tolerant quantum repeaters with minimal physical resources and implementations based on single-photon emitters *Phys. Rev.* A **72** 052330

[10] Jelezko F, Gaebel T, Popa I, Gruber A and Wrachtrup J 2004 Observation of coherent oscillations in a single electron spin *Phys. Rev. Lett.* **92** 076401

[11] Jelezko F, Gaebel T, Popa I, Domhan M, Gruber A and Wrachtrup J 2004 Observation of coherent oscillation of a single nuclear spin and realization of a two-qubit conditional quantum gate *Phys. Rev. Lett.* **93** 130501

[12] Gurudev Dutt, Childress L, Jiang L, Togan E, Maze J, Jelezko F, Zibrov A S, Hemmer P R and Lukin M D 2007 Quantum register based on individual electronic and nuclear spin qubits in diamond *Science* **316** 1312–6

[13] Neumann P *et al* 2010 Quantum register based on coupled electron spins in a room-temperature solid *Nat. Phys.* **6** 249–53

[14] Togan E *et al* 2010 Quantum entanglement between an optical photon and a solid-state qubit *Nature* **466** 730–5

[15] Maze J R *et al* 2008 Nanoscale magnetic sensing with an individual electronic spin in diamond *Nature* **455** 644–8

[16] Balasubramanian G *et al* 2008 Nanoscale imaging magnetometry with diamond spins under ambient conditions *Nature* **455** 648–52

[17] Taylor J M, Cappellaro P, Childress L, Jiang L, Budker D, Hemmer P R, Yacoby A, Walsworth R and Lukin M D 2008 High-sensitivity diamond magnetometer with nanoscale resolution *Nat. Phys.* **4** 810–6

[18] Weber J R, Koehl W F, Varley J B, Janotti A, Buckley B B, Walle C G V D and Awschalom D D 2010 Quantum computing with defects *Proc. Natl Acad. Sci.* **107** 8513–8

[19] Schietinger S, Barth M, Aichele T and Benson O 2009 Plasmon-enhanced single photon emission from a nanoassembled metal/diamond hybrid structure at room temperature *Nano Lett.* **9** 1694–8

[20] Hadden J P, Harrison J P, Stanley-Clarke A C, Marseglia L, Ho Y-L D, Patton B R, O'Brien J L and Rarity J G 2010 Strongly enhanced photon collection from diamond defect centres under micro-fabricated integrated solid immersion lenses arXiv:1006.2093

[21] Park Y-S, Cook A K and Wang H 2006 Cavity QED with diamond nanocrystals and silica microspheres *Nano Lett.* **6** 2075–79
[22] Larsson M, Dinyari K N and Wang H 2009 Composite optical microcavity of diamond nanopillar and silica microsphere *Nano Lett.* **9** 1447–50
[23] Fu K-M C, Santori C, Barclay P E, Aharonovich I, Prawer S, Meyer N, Holm A M and Beausoleil R G 2008 Coupling of nitrogen-vacancy centers in diamond to a GaP waveguide *Appl. Phys. Lett.* **93** 234107
[24] Barclay P E, Fu K-M C, Santori C and Beausoleil R G 2009 Chip-based microcavities coupled to nitrogen-vacancy centers in single crystal diamond *Appl. Phys. Lett.* **95** 191115
[25] Englund D, Shields B, Rivoire K, Hatami F, Vuckovic J, Park H and Lukin M D 2010 Deterministic coupling of a single nitrogen vacancy center to a photonic crystal cavity *Nano Lett.* **10** 3922–6
[26] van der Sar T, Hagemeier J, Pfaff W, Heeres E C, Oosterkamp T H, Bouwmeester D and Hanson R 2010 Deterministic nano-assembly of a coupled quantum emitter-photonic crystal cavity system arXiv:1008.4097
[27] Gruber A, Drabenstedt A, Tietz C, Fleury L, Wrachtrup J and Borczyskowski C 1997 Scanning confocal optical microscopy and magnetic resonance on single defect centers *Science* **276** 2012–4
[28] Rabeau J R, Reichert P, Tamanyan G, Jamieson D N, Prawer S, Jelezko F, Gaebel T, Popa I, Domhan M and Wrachtrup J 2006 Implantation of labelled single nitrogen vacancy centers in diamond using 15N *Appl. Phys. Lett.* **88** 023113
[29] Meijer J, Burchard B, Domhan M, Wittmann C, Gaebel T, Popa I, Jelezko F and Wrachtrup J 2005 Generation of single color centers by focused nitrogen implantation *Appl. Phys. Lett.* **87** 261909
[30] Meijer J *et al* 2008 Towards the implanting of ion and positioning of nanoparticles with nm spatial resolution *Appl. Phys.* A **91** 567–71
[31] Toyli D M, Weis C D, Fuchs G D, Schenkel T and Awschalom D D 2010 Chip-scale nanofabrication of single spins and spin arrays in diamond *Nano Lett.* **10** 3168–72
[32] Hausmann B, Khan M, Zhang Y, Babinec T, Martinick K, McCutcheon M, Hemmer P and Loncar M 2010 Fabrication of diamond nanowires for quantum information processing applications *Diam. Relat. Mater.* **19** 621–9
[33] Ziegler J F, Ziegler M D and Biersack J P 2008 *SRIM—The stopping range of ions in matter* www.SRIM.org
[34] Shen Y, Sweeney T M and Wang H 2008 Zero-phonon linewidth of single nitrogen vacancy centers in diamond nanocrystals *Phys. Rev.* B **77** 033201
[35] Jelezko F 2010 private communication
[36] Hausmann B J M, Bulu I, Babinec T M, Khan M, Hemmer P and Loncar M 2010 Top-down fabricated hybrid diamond-plasmon nanoparticles *Conf. on Lasers and Electro-Optics, OSA Technical Digest* (Optical Society of America) paper CMFF3 (CD)
[37] Barclay P E, Fu K-M, Santori C and Beausoleil R G 2009 Hybrid photonic crystal cavity and waveguide for coupling to diamond NV centers *Opt. Express* **17** 9588–601
[38] McCutcheon M W and Lončar M 2008 Design of a silicon nitride photonic crystal nanocavity with a quality factor of one million for coupling to a diamond nanocrystal *Opt. Express.* **16** 19136–45
[39] Englund D, Shields B, Rivoire K, Hatami R, Vuckovic J, Park H and Lukin M D 2010 Deterministic coupling of a single nitrogen vacancy center to a photonic crystal nanocavity arXiv:1005.2204
[40] Batalov A, Zierl C, Gaebel T, Neumann P, Chan I-Y, Balasubramanian G, Hemmer P R, Jelezko F and Wrachtrup J 2008 Temporal coherence of photons emitted by single nitrogen-vacancy defect centers in diamond using optical Rabi-oscillations *Phys. Rev. Lett.* **100** 077401